

5G RF Front End Module Architectures for Mobile Applications

Florinel Balteanu, Hardik Modi, Yunyoung Choi, Junhyung Lee, Serge Drogi, Sabah Khesbak

Skyworks Solutions Inc., CA92617, USA

florinel.balteanu@skyworksin.com

Abstract — The explosive growth and adoption of smartphones provides access to voice and data for billions of people worldwide today and connected devices are expected to reach 5.6 billion in 2020. This growth has been and continues to be the engine for semiconductor industry due to required computational power of CMOS technology in lower feature nodes as FinFet 7nm/14nm for application processors, modems and transceivers. The adoption of 5G will bring higher data capacity and low latency using sub-6GHz bands and mmWave spectrum, with the first expected to be deployed in next generation 5G smartphones. This 5G evolution will open up new applications where our phones will be a conduit for massive amounts of data. With lower feature nodes for RF CMOS there is an increased usage of digital signal processing (DSP) and RF digital calibration which are part of modern modem technology. 5G requires more RF bands, so there is a clear shift in terms of what parts of the RF systems are portioned in advanced CMOS nodes and what RF and analogue blocks are integrated with other components such as acoustic duplexers and filters in multiple RF front-end-modules (RF FEMs). This paper proposes a low cost RF partitioning and architecture which will be part of 5G RF FEMs. This paper also presents some design/measurement results and explains how these modules can be integrated into a complex 4G/5G system RF front end (RFFE) for mobile applications.

Keywords — RF front end (RFFE), CMOS, GaAs, SiGe, silicon on insulator (SOI), SAW, BAW, GSM, 3G, 4G, 5G, GPS, ultra-wide band (UWB), long term evolution (LTE), LTE advanced, WiFi 6, power amplifier (PA), envelope tracking (ET), multimode multiband power amplifier (MMBPA), frequency duplex division (FDD), time division duplex (TDD), digital signal processing (DSP), MIMO, transmit (Tx), multi-chip-module (MCM), carrier aggregation (CA), licensed-assisted access (LAA), enhanced LAA (eLAA), high power user equipment (HPUE), duplexer, filter, diplexer, RF switch, power management IC (PMIC), ACLR, EVM.

I. INTRODUCTION

The need for high data rates in mobile applications together with the demand for new applications is pushing the adoption for WiFi 6 [1] and 5G long term evolution (LTE) [2]. Both will provide the new mobile applications with fast and low latency data for ultra-reliable and low latency communications (URLLC) services. Together with other RF technologies such as ultra-wide band (UWB) [3], 5G will enable other services, for example vehicle-to-everything (V2X) communications. Low latency in mobile networks is a critical requirement for making autonomous vehicles safe. For new features in 5G, mobile devices such as smartphones will be a conduit for a cloud of applications. Next generation 5G

smartphones need to support legacy voice (2G/3G) capabilities and enable the seamless transition from 4G to 5G. To provide more RF spectrum, new bands have been allocated for 5G as presented in Fig.1 and 3G/4G bands will be re-farmed for 5G.

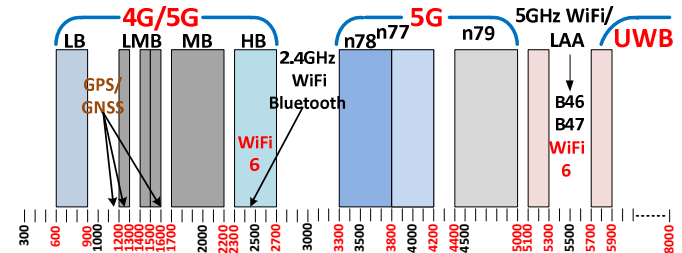


Fig. 1. 4G/5G and WiFi 6 spectrum.

The transition from the 3G/4G FEMs to 5G FEMs poses the following challenges:

- Wider channel bandwidth up to 100 MHz where new techniques for envelope tracking are required.
- High power user equipment (HPUE) requires 26 dBm at the antenna port.
- Higher peak to power ratio waveforms for uplink (UL) such as 256 QAM; this requires more power amplifier back-off with lower distortions and noise.
- Cost efficient and compact size for 2x2 UL-MIMO and downlink (DL) data rate coverage.
- LAA and eLAA will be introduced as part of 5G as a possibility for bandwidth aggregation with a licensed anchor LTE band in UL and DL.
- New 5G dedicated bands for sub-6 GHz such as n77/n78 (3.3-4.2 GHz), n79 (4.4-4.5 GHz) and eLAA bands B46, B47.
- Intra-band coexistence with 3G/4G bands in 5G re-farmed bands.
- Dual-SIM operation for voice under 2G (GSM) and data (3G/4G/5G) which will increase the linearity requirements for antenna switches.
- Increased number of antennas to 6-8. The requirement is to reach these antennas from different LTE radios which have to coexist with multiple WiFi & WiFi 6 radios, Bluetooth, GPS and UWB.

To meet these challenges, low cost and high linearity RFEs together with multiple filters are required to access

multiple antennas for 4G/5G mobile devices as shown in Fig. 2.

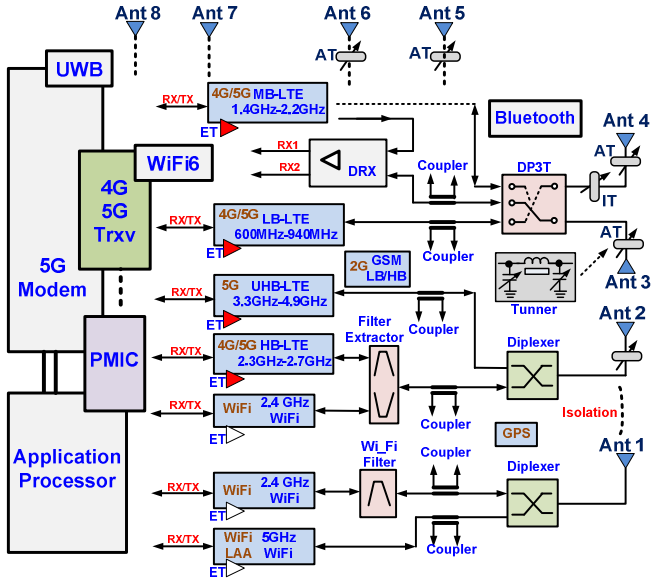


Fig. 2. Sub-6GHz 4G/5G RFFE structure for a mobile device.

The 3GPP standard body requires LTE power delivered at the antenna to be 23 dBm. 5G implementation results in power losses from filter/duplexers, switches, diplexers, board and Impedance/Aperture Tuners (IT, AT) and the PA is required to deliver at least 27-28 dBm assuming less than 4-5dB total losses. Also for LTE 5G, there is an increase from 20 MHz to 40 MHz/0 MHz for the modulation uplink bandwidth in low/mid bands as well an increase of the output power for HPUE to 26 dBm. There is also an increase in modulation bandwidth up to 100 MHz for high/ultrahigh 5G bands such as new bands n77/n78 and n79. The goal of 5G is to reach a transmission capacity of 1 Gbps. The capacity of a wireless system is shown by Shannon formula as

$$C = B_w \sum_{k=1}^k \log_2 \left(1 + \frac{S_k}{N_x + I_k} \right) \quad (1)$$

To achieve higher capacity following Eq.1 these are the techniques which are incorporated in 5G:

- increase channel bandwidth B_w ; eg 100 MHz LTE
- increase spatial multiplexing level k through MIMO
- increase the transmit power; such as HPUE
- decrease noise N_x and improve receive sensitivity
- reduce in band interference on link k , especially in multiple UL Tx such as CA and MIMO
- higher order modulation such as 256QAM for UL

II. 4G/5G FRONT END MODULE STRUCTURE

To meet 5G geographical coverage requirements, smartphones will need to cover more than 50 bands from 600 MHz to 6 GHz. In parallel, there are other radios and bands used at the same time such as WiFi/WiFi6 (2.4 GHz/5 GHz), UWB (6-8 GHz), GPS (1.17 GHz-1.5 GHz), Bluetooth (2.4 GHz) and NFC(13.56 kHz). Sub-3 GHz bands provides primary cellular coverage and 3G/4G bands will be re-farmed

to 4.5G/5G and the 3 GHz new 5G bands will provide the primary capacity layer with multiple MIMO. All these radios will need to share common antennas without jamming the other device radios. In addition, old features such as 2G GSM need to be supported together with the new features introduced in 5G such as LAA and eLAA which use 5 GHz unlicensed band as bandwidth aggregation with a licensed LTE anchor, usually in low band (LB). There has been a lot of research on single die power amplifier in different technologies such as SiGe, CMOS and SOI [4-5]. However, with band proliferation and coexistence requirements, the biggest share and cost is determined by the acoustic filters which are placed together with band and antenna SOI switches into a FEM with integrated duplexers (FEMiD) and filters (FEMiF) for TDD space, as shown in Fig. 3.

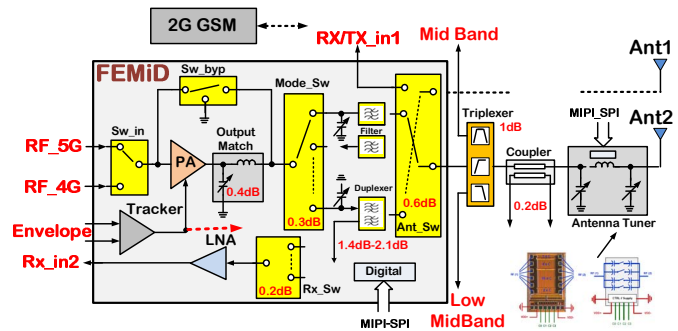


Fig. 3. Sub-6GHz 4G/5G FEMiD architecture.

These LTE modules can include two to three PAs and 10-12 SAW and BAW filters [6]. Also WiFi modules include BAW filters for coexistence with LTE high bands as presented in Fig. 4.

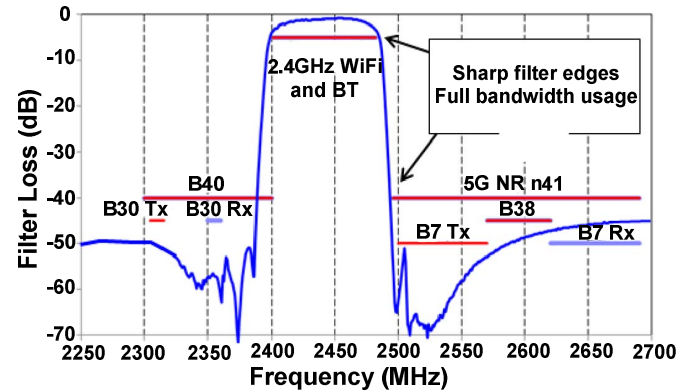


Fig.4. WiFi 2.4GHz BAW coexistence filter characteristic.

The RF power amplifier is one of the most critical components within the transmitter chain due to efficiency and linearity requirements. The linearity requirements for LTE are expressed by adjacent channel leakage power ratio (ACLR) and for 5G EVM become a critical parameter for UL 256 QAM. Doherty power amplifiers [7] and envelope tracking [8] (ET) have been extensively researched and used techniques to meet the efficiency and linearity requirements. Doherty power

amplifier provides high efficiency and is used in base-stations but is less used in mobile applications due to broadband limitation and load mismatch operation [9]. In mobile applications such smartphones, ET is used with a broadband PA with class E output match and typically with two stages [10-11], as shown in Fig. 5.

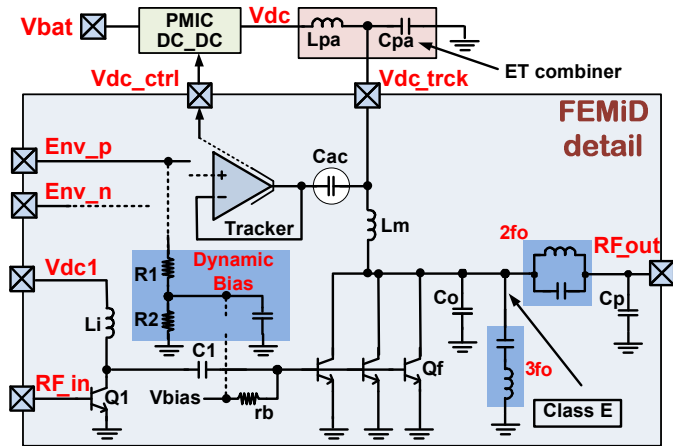


Fig. 5. 5G tracker and power amplifier for mobile application.

III. ENVELOPE TRACKING

4G smartphones have just one ET circuit which can provide V_{dc} tracked to one PA/FEM at a time. With the migration to 5G (where more than two transmit PAs are active at a time) there is the need to place the ET error amplifier (tracker) inside of the FEMiD and to have a general PMIC which provides 4-5 V_{dc} power domains. For a typical linear PA operating in class B mode when the active device conducts 180° the maximum output power P_{out_max} is given by

$$P_{out_max} = \frac{(V_{dd} - V_{kn})^2}{2Rl_{opt}} \quad (2)$$

where Rl_{opt} is the optimum impedance which has to be matched at the output load through the marching network and V_{kn} is the knee voltage for the output transistor. Under ET the instantaneous supply voltage V_{dc} for the last stage is provided by ET. Around 80% of the energy is delivered by the DC-DC and the rest by the error amplifier (tracker) presented in Fig. 6.

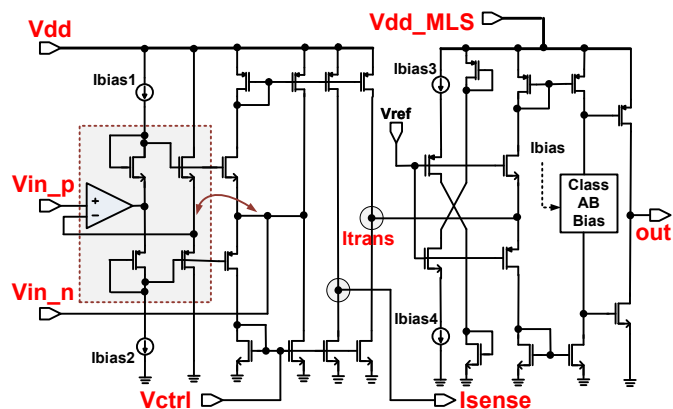


Fig. 6. Current mode error amplifier (tracker).

For 5G, the error amplifier is required to deliver increased peak voltage due to an increase in the peak-to-average-ratio (PAPR)

$$PAPR = 20 \log \left(\frac{V_{dc_trck_peak}}{V_{dc_trck_rms}} \right) \quad (3)$$

To reduce the peak voltage requirement and to keep the load line to reasonable values in HPUE case, the power amplifier can be split into two identical structures, independently tracked. The outputs can be combined using a RF Wilkinson combiner. A PA structure with two or more identical tracked structure can also use a balun to cancel second harmonic which is a coexistence issue for multiple 5G transmitters.

IV. SOI SWITCH CONTROL

The FEMiD and FEMiF include many SOI switches. Together with the LNAs these switches are integrated on several SOI dies to provide enough isolation. The insertion loss (IL) and input intercept point (IIP3) for a series-shunt switch are defined by the relations

$$IL = 10 \log \left[\left(1 + \frac{Ron}{2Zo} \right)^2 + \left(\frac{2\pi C_{off} (Ron + Zo)}{2} \right)^2 \right] \quad (4)$$

$$IIP3 = 10 \log \left(\frac{Isat^2 (Ron + 2Zo)^4}{4RonZo^2} \right) + 30 \quad (5)$$

Where Ron is the on-state channel resistance on the switch

$$Ron = n \frac{1}{\mu Cox \frac{w}{l} (V_{pos} - V_{th})} \quad (6)$$

V_{pos} is the voltage applied to turn on the series switch and n define the number of series switches. To improve switch performance, one method is to overdrive through V_{pos} voltage increase and also to track the V_{pos} with the instantaneous power given by ET signal which is available for the FEMiD as presented in Fig. 7. Also, several clock phases are used to reduce the charge pump clock feedthrough into SOI switches.

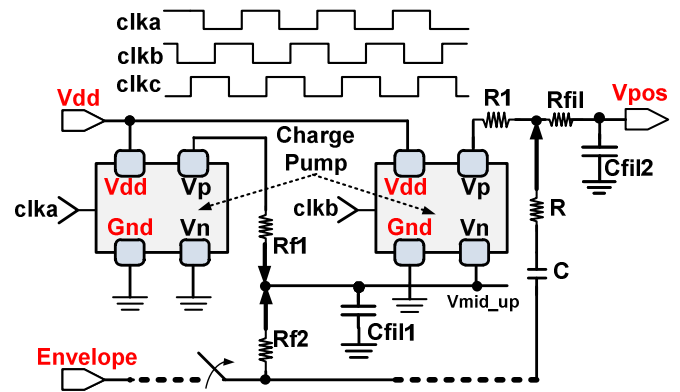


Fig. 7. SOI Switch- V_{pos} schematic.

V. MEASUREMENTS

The conversion from 4G RFFE to 5G is an evolutionary transition with many circuits/filters reused and some designed especially for 5G. The progress is possible also due to more

components packaged into a smaller space [12, 13]. The high bandwidth tracker as shown in Fig. 6 has been integrated into a dual-gate 0.18 μ m CMOS technology together with the GaAs CMOS controller and tested. Fig. 8 presents the voltage swing for the error amplifier into PA $R_{load}=6$ ohm and $C_{pa}=120$ pF for three tones 1 MHz, 84 MHz and 85 MHz.

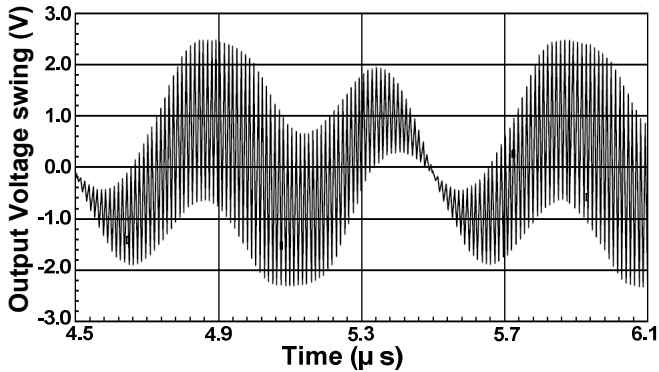


Fig. 8. Error amplifier voltage swing (4.8V) for $V_{dd}=5.5V$ and $I_{cq}=30mA$.

Fig. 9 presents the waterfall curves for 3.5 GHz, n78 5G band for different voltage supplies. The new bands n77, n78 and n79 will provide more spectrum and higher bandwidth (up to 100 MHz). For 80 MHz LTE bandwidth the overall efficiency for n78 PA and tracker is 32%, with -37 dBc ACLR1.

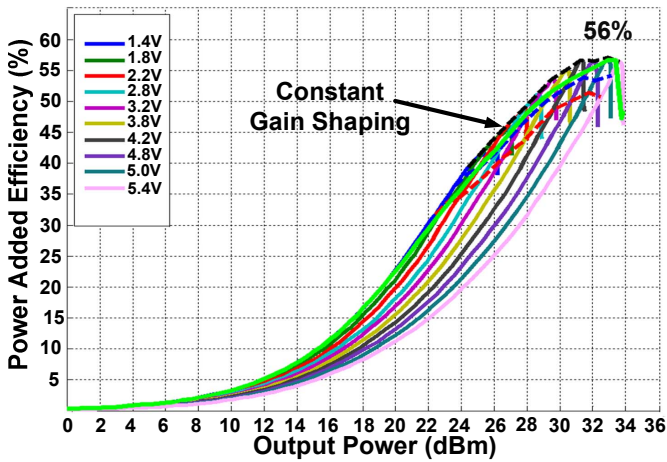


Fig. 9. Waterfall curves for n78 band 3.5GHz GaAs PA.

5G RFFE will use several uplink Tx (GSM/LTE) operating the same time and one of the main problems is the internal noise mitigation in receive bands, especially for GSM receive bands. Fig. 10 shows the DP3T SOI Switch and Fig. 11 presents the noise reduction using the proposed SOI charge pump shown in Fig. 7.

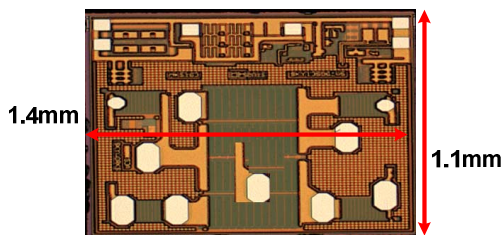


Fig. 10. DP3T Antenna switch photograph.

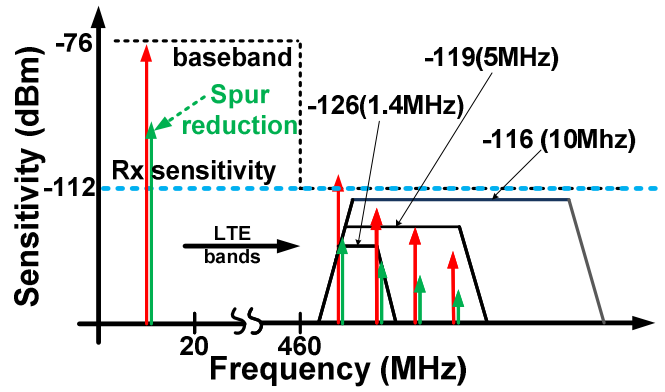


Fig. 11. Clock feed-through spur reduction for 5G SOI switches.

VI. CONCLUSIONS

Fully integrated 5G RFFE architectures are presented. The transition from 3G/4G to 5G, especially for very large volume products such as smartphones, is an evolutionary process. This paper presents and characterizes few novel circuits such as high bandwidth ET, 5G new band (n78) power amplifier and SOI switch control for lower noise and high linearity. These will enable the 5G RFFE adoption and integration.

REFERENCES

- [1] Wi-Fi Alliance introduces Wi-Fi 6, www.wi-fi.org, Oct. 2018.
- [2] D. Pehlke, D. Brunel, K. Walsh, S. Kovacic, "Sub-6GHz 5G for UE, Optimizing Cell Edge User Experience," *IWPC 4G/5G Multi-band, Multi-Mode User Equipment*, Austin, October 2017.
- [3] I. Dotlic, A. Connell, H. Ma, J. Clancy, M. McLaughlin, "Angle of Arrival Estimation Using Decawave DW1000 Integrated Circuits", *14th Positioning Navigation and Communications (WPNC) Workshop*, 2017, pp. 1-6.
- [4] D.Y.C. Lie, J. Tsay, T. Hall, T. Nukala and J. Lopez, "High-Efficiency Silicon RF Power Amplifier Design – Current Status and Future Outlook," in *IEEE international Symposium on Radio-Frequency Integration Technology (RFIT) Dig.*, August 2016, pp. 1–3.
- [5] F. Balteanu, "Linear Front End Module for 4G/5G LTE Advanced Applications," *48th European Microwave Conference (EuMC)*, 2018, pp. 251-254.
- [6] *Qorvo Investor Day*, Qorvo, May 23rd, 2018.
- [7] W. H. Doherty, "A new high efficiency power amplifier for modulated waves," *Proc. Inst. Radio Eng.*, vol. 24, no. 9, pp. 1163–1182, September 1936.
- [8] L.R. Kahn, "Single-sideband transmission by envelope elimination and restoration," *Proc. Inst. Radio Eng.*, vol. 40, no. 7, pp. 803-806, July 1952.
- [9] E. Zenteno, M. Isaksson, and P. Händel, "Output Impedance Mismatch Effects on the Linearity Performance of Digitally Predistorted Power Amplifiers," *IEEE Transactions on Microwave Theory and Techniques*, vol. 63, no. 2, pp. 754-765, Feb 2015.
- [10] P. Asbeck and Z. Popovic, "ET Comes of Age." *IEEE Microwave Magazine*, vol17, no.3, pp. 16-25, March 2016.
- [11] A. Grebennikov, N.O. Sokal and M.J. Franco, *Switchmode RF and Microwave Power Amplifiers*, New York, NY: Academic Press, 2012.
- [12] A. Bisogin, N. Nachabe, C. Luxey, F. Gianesello, D. Gloria, J.R. Costa, C.A. Fernandes, Y. Alvarez, A.Arboleya, J. Laviada, F.Las-Heras, N. Dolatsha, B. Grave, M. Sawaby, A. Arbabian, "Ball Grid Array Module With Integrated for 5G Backhaul/Fronthaul Communications in F-Band," *IEEE Transactions on Antennas and Propagation*, vol. 65, no. 12, pp. 6380-6394, December 2017.
- [13] R. Darveaux, H. Chen, S. Branchevsky and M. Harsha, "As-shipped vs. Mounted Height for BGA and LGA Packages," *2018 SMTA Conference*, 2018, pp.1-4.